

Chiral nihility effects on energy flow in chiral materials

Cheng-Wei Qiu,^{1,2} Nawaz Burokur,¹ Saïd Zouhd,¹ and Le-Wei Li^{2,*}

¹Laboratoire de Génie Electrique de Paris, CNRS Ecole Supérieure D'Électricité, Plateau de Moulon 91192, Gif-Sur-Yvette, France

²Nanoscience & Nanotechnology Initiative and Department of Electrical & Computer Engineering, National University of Singapore, Kent Ridge, Singapore 119260

*Corresponding author: lwli@nus.edu.sg

Received August 28, 2007; revised October 19, 2007; accepted October 22, 2007;
posted October 31, 2007 (Doc. ID 86923); published December 5, 2007

The propagation of electromagnetic plane waves in an isotropic chiral medium is characterized, and a special interest is shown in chiral nihility and the effects of chirality on energy transmission. In particular, the wave impedance is matched to that of free space. Moreover, the refractive index n is also matched in impedance to that of free space when an appropriate value of the chirality is chosen. A “chiral nihility” medium is explored in which both the permittivity and the permeability tend to zero. Some specific case studies of chiral nihility are presented, and Brewster angles are found to cover an extremely wide range. The E -field distributions in these different cases where the chiral slab is placed in free space are analyzed by using the appropriate constitutive relations. It is shown from numerical calculations that one can obtain some critical characteristics of the effects of chirality on energy transmission and reflection, such as transparency and power tunneling.

© 2007 Optical Society of America
OCIS codes: 260.2065, 160.1585.

1. INTRODUCTION

In 1968, Veselago theoretically demonstrated the electromagnetic properties of substances with simultaneously negative permittivity ϵ and permeability μ [1]. A material possessing these properties is now referred to as a left-handed material, since the electric field \mathbf{E} , magnetic field \mathbf{H} , and the wave vector \mathbf{k} in the medium obey a left-handed rule. Left-handed materials possess some unique properties compared with conventional dielectric materials, such as a negative refractive index [2], subwavelength imaging [3], a backward-wave region [4], and double-negative parameters [5]; therefore these media are also often referred to as negative refractive index materials. This kind of medium does not, however, normally exist in nature. In particular, the negative μ value is not found in natural materials.

Thirty years later, Pendry and co-workers revisited the negative refractive index material problem and developed the concept of a perfect lens using the double-negative constitutive parameters, ϵ and μ [6]. The first metamaterial prediction by Veselago and its later formulation by Pendry were both theoretical. The research work in this area was not pushed that far until Pendry proposed the structure of split-ring resonator [7] and Shelby *et al.* experimentally realized a left-handed material for the first time, where measurements confirmed negative refraction in the microwave region [8]. However, it is a very difficult task to realize negative permeability from metallic split-ring resonators and to achieve low-loss double-negative media at much higher frequencies. A recent publication on metamaterials in the visible region showed that negative values of the real parts of the permeability and the

permittivity can be obtained simultaneously, but a negative index of refraction cannot be achieved because of high values of the imaginary part of the permeability [9].

On the other hand, negative refraction can be also achieved by using chiral media [10–13], which belong to a general class of bianisotropic media. The use of a chiral medium can help considerably for achieving negative refraction in the optical region [14–16] where artificial magnetic materials become unnecessary. In chiral media with inclusions of long helices, a backward wave can be excited along the helix, which acts as a delay line. Electric or magnetic excitation will simultaneously produce both electric and magnetic polarizations [17,18]. In this paper, we deal with the propagation of electromagnetic plane waves in chiral nihility media. Cases of chiral nihility where both the relative permittivity ϵ_r and the relative permeability μ_r are very small will be considered. The possibility of matching the refractive index n and the wave impedance Z to those of free space will be discussed. Z is matched when both the permittivity and the permeability take the same values, and n is matched according to the different values of ϵ_r , μ_r , and κ . This type of medium also favors the realization of a negative refraction and the propagation of backward waves when the chirality parameter is appropriately chosen.

In this paper, we investigate eigenwaves propagating in a chiral medium. The reflection from a dielectric–chiral interface and wave propagation in an infinite chiral slab placed in free space are discussed. The E -field is analyzed, and related results established by numerical calculations are presented at different angles of incidence and for different sets of values of the constitutive parameters.

2. SEMI-INFINITE CHIRAL MEDIA

In this section, we consider a plane wave incident upon the interface between an achiral dielectric medium and a chiral medium as shown in Fig. 1. The Cartesian coordinate system (x, y, z) is employed, and the x - y plane is considered the plane of interface between the dielectric (permittivity ϵ_1 and permeability μ_1) and a homogeneous chiral medium.

The constitutive relations used for the chiral medium are defined as [19,20]

$$\mathbf{D} = \epsilon_r \epsilon_0 \mathbf{E} - i \kappa \sqrt{\epsilon_0 \mu_0} \mathbf{H}, \quad (1)$$

$$\mathbf{B} = \mu_r \mu_0 \mathbf{H} + i \kappa \sqrt{\epsilon_0 \mu_0} \mathbf{E}. \quad (2)$$

A monochromatic time-harmonic variation $\exp(i\omega t)$ is assumed throughout this paper, but omitted. From the source-free Maxwell's equations, we have the following time-harmonic forms:

$$\nabla \times \mathbf{E} = -i\omega \mathbf{B}, \quad (3)$$

$$\nabla \times \mathbf{H} = i\omega \mathbf{D}. \quad (4)$$

The chiral medium is isotropic, and we assume that a monochromatic plane wave propagates along the z axis of the Cartesian system (x, y, z) where the unit vectors are $(\hat{e}_x, \hat{e}_y, \hat{e}_z)$ as illustrated in Fig. 1. The wavenumbers of the two eigenwaves in the chiral medium then read as

$$k_{1,2} = k_0(\sqrt{\mu_r \epsilon_r} \pm \kappa), \quad (5)$$

where k_0 denotes the wavenumber in vacuum.

In a chiral medium, two eigenmodes exist, and they propagate at different phase velocities of ω/k_1 and ω/k_2 . The E -fields associated with these two eigenmodes can be expressed by

$$\mathbf{E}_1 = \mathbf{E}_{01}(\hat{e}_x + i\hat{e}_y)\exp(-ik_1z), \quad (6)$$

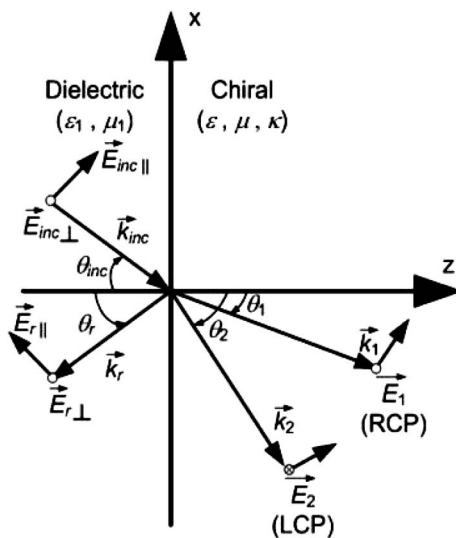


Fig. 1. Orientation of the wave vectors at an oblique incidence on a dielectric-chiral interface. The subscripts \parallel and \perp , respectively, stand for parallel and perpendicular with respect to the plane of incidence.

$$\mathbf{E}_2 = \mathbf{E}_{02}(\hat{e}_x - i\hat{e}_y)\exp(-ik_2z), \quad (7)$$

which correspond to right-handed and left-handed circularly polarized waves, respectively. The refractive indices are thus given as

$$n_{1,2} = \sqrt{\mu_r \epsilon_r} \pm \kappa. \quad (8)$$

Potential applications in phase compensator and quantum devices can be envisaged for chiral media, since one of the refractive indices can be fairly small, leading to a quantum vacuum that is highly discretized [21]. If a proper model is applied to characterize the chiral media, one will further obtain dispersive refractive indices. Thus, each of the refractive indices can be zero at a certain frequency [22].

In order to study the reflected power at the interface between the dielectric medium and the chiral medium, the following boundary conditions have to be satisfied:

$$\hat{z} \times [\mathbf{E}_{inc} + \mathbf{E}_r] = \hat{z} \times [\mathbf{E}_1 + \mathbf{E}_2], \quad (9)$$

$$\hat{z} \times [\mathbf{H}_{inc} + \mathbf{H}_r] = \hat{z} \times [\mathbf{H}_1 + \mathbf{H}_2]. \quad (10)$$

The method used by Silverman for retrieving Fresnel reflection and transmission coefficients (see Sect. 3 of [23]) is adopted (but will not be repeated here). They are further transformed into the Tellegen formalism. In Fig. 2, the reflected power versus the angle of incidence is drawn for two different configurations.

The first case deals with a chiral medium where the permittivity is greater than that of the dielectric. There then exists a Brewster angle for an incidence at about 65° for parallel polarization, as shown in Fig. 2(a). For the second case, shown in Fig. 2(b), the chiral medium has a lower permittivity than the surrounding dielectric. For the value of $\kappa=0.25$, no Brewster angle can be observed for either polarization of the incident field. When $\theta=20^\circ$, however, the reflected power of P_{\parallel} has a minimum, which is close to zero. Total reflection is thus obtained from the 39° incidence for both $P_{pa(\parallel)}$ and $P_{pe(\perp)}$ polarizations. Further investigation reveals that the permittivity ratio (i.e., the permittivity of the dielectric over the permittivity of the chiral medium) determines the zero and total reflection characteristics. The zero reflection occurs only for parallel polarization, which is consistent with the results related to the conventional dielectric-dielectric interface. It is interesting to observe that the total reflection happens over a wide range of incident angles, and a secondary total-reflection angle at $\theta=22^\circ$ appears at the perpendicular polarization.

In what follows, we investigate the energy flow from the dielectric to the chiral nihility in Fig. 3, where some interesting phenomena arise.

Two cases of chiral nihility are considered, i.e., in the presence and absence of impedance matching to the air. It is easily found by comparing Fig. 3(a) with Fig. 2(a) that a zero-reflection angle occurs at the perpendicular polarization instead of the parallel polarization, which is in contrast to the situation for normal chiral or dielectric materials. It is shown that the reflected power varies drastically with the incident angle within a certain range. The zero-reflection angle at 27° is quite close to the lowest

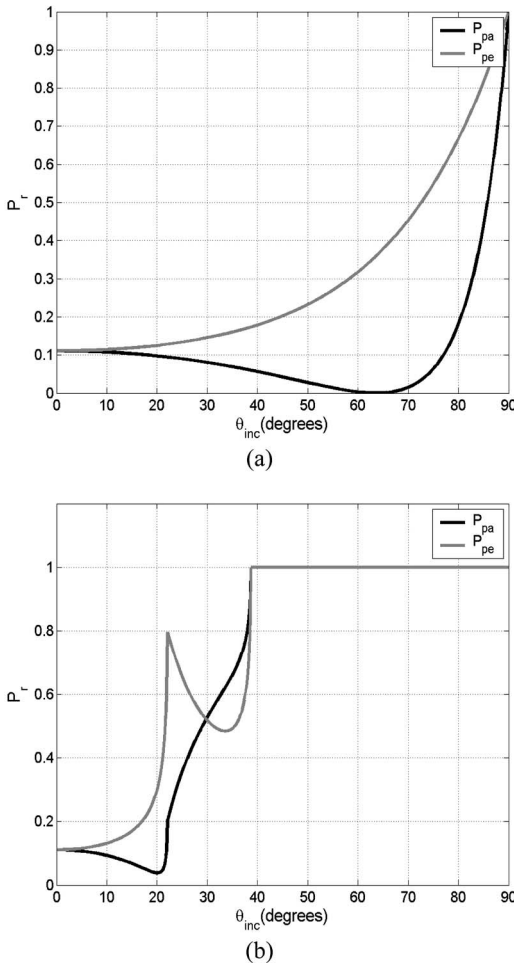


Fig. 2. Reflected power as a function of the incidence with unit permeability, the same chirality, but different permittivity. $\mu_1 = \mu = 1$, $\kappa = 0.25$. (a) $\epsilon_1 = 1$, $\epsilon = 4$; (b) $\epsilon_1 = 4$, $\epsilon = 1$.

total reflection angle at 30° , which means that this range is quite angle sensitive. More surprisingly, the dependence of reflected power on the incidence becomes identical for both polarizations when the impedance of chiral nihility is matched to that of free space. In this special case, the Brewster angle forms a range instead of a single angle as shown in Fig. 3(b), and total reflection happens when the incident angle is greater than 30° , although impedance matching is achieved. The reflection is due to the mismatch of the refractive indices.

As one can see, the chirality in each case in Fig. 3 is doubled in Fig. 4, if we keep other parameters unchanged. The chiral effects of chiral nihility are presented. In Fig. 4, the reflected powers at both polarizations carry a similar dependence on incidence, while the magnitude of reflected power significantly differs from that in Fig. 3.

In Fig. 4, the reflected power is quite stable over the whole region except at 90° . If the impedance of chiral nihility is matched, the value will be further reduced to zero [see Fig. 4(b)], which means that the Brewster angle covers almost the whole range of incident angles. Therefore, under such circumstances, all the energy is transmitted to the chiral nihility except at a parallel incidence. This outcome may be of great importance for realizing imaging

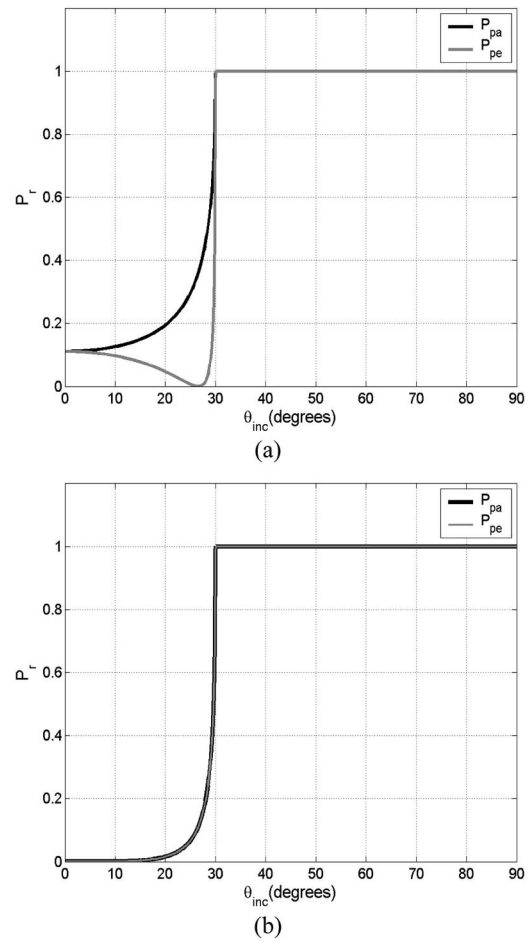


Fig. 3. Reflected power as a function of the incidence with different cases of chiral nihility. $\kappa = 0.5$. (a) $\epsilon_1 = \mu_1 = 1$, $\epsilon = 4 \times 10^{-5}$, $\mu = 1 \times 10^{-5}$; (b) $\epsilon_1 = \mu_1$, $\epsilon = \mu = 1 \times 10^{-5}$.

characteristics without much loss of information with a point source or a line source, since one of the refractive indices of chiral nihility is very close to -1 .

Figure 5 shows the reflected power versus the chirality for the same two configurations as above at an oblique incidence of 45° . When the chiral medium is denser than the dielectric [Fig. 5(a)], the reflected power shows a maximum of 0.8 for $\kappa = 2$ for perpendicular polarization of the incident field and tends to a stable value of 0.22 for $\kappa > 4$. For parallel polarization, two maxima are obtained ($P_r = 0.8$) at $\kappa = 1.29$ and $\kappa = 2.71$, respectively. In order to have good transmission through the interface, the chirality must be either lower than 1.29 or greater than 2.71.

In contrast, when the dielectric is denser than the chiral medium [Fig. 5(b)], total reflection is observed at both polarizations for a chirality smaller than 0.42. In the case of parallel polarization, the reflected power decreases to a stable value of 0.22 as the chirality increases. At the perpendicular polarization of the incident field, a minimum is first observed for $\kappa = 1$, and then another maximum is observed for $\kappa = 2.41$. When $\kappa > 3$, the reflected power tends to 0.04. If we further increase the mismatching of the permittivity between the dielectric and the chiral medium, the variational curves shown in Fig. 5 shift to the right (higher values of chirality), and the amplitude of the reflected power increases.

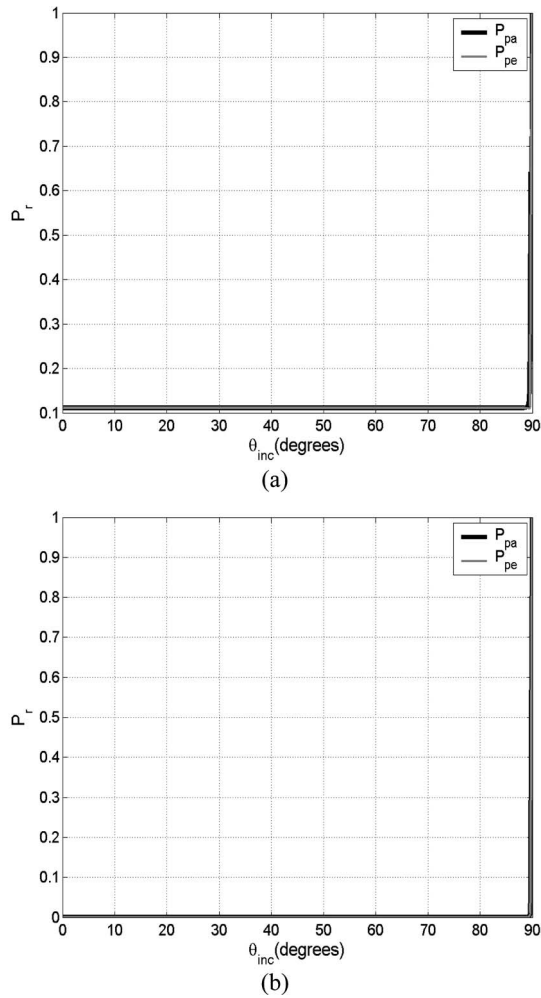


Fig. 4. Reflected power as a function of the incidence with the same permittivity and permeability as in Fig. 3 but with a higher chirality. $\epsilon_1 = \mu_1 = 1$, $\epsilon = 4 \times 10^{-5}$, $\mu = 1 \times 10^{-5}$, $\kappa = 1$.

In contrast to the normal chiral slab, chiral nihility slabs at an oblique incidence are also studied in Fig. 6. Similarly, particular values of chirality will lead to zero reflection; these values represent the so-called critical chirality κ_c . In Fig. 6(a), $\kappa_c \approx 0.75$, which exists only for perpendicular polarization. If the chirality is lower than κ_c , total reflection happens, and no power can be transmitted to the chiral nihility slab. When the chirality is sufficiently large, the reflected powers approach their respective stable values. It is found that the stable reflected power of P_{\parallel} is about 7 times larger than that of P_{\perp} . If the chiral nihility slab has its impedance matched to the free space, both P_{\parallel} and P_{\perp} have identical performance versus the chirality, and κ_c can be observed for both cases. This suggests that higher chirality would be a better choice if energy transport is desired.

3. INFINITE CHIRAL NIHILITY SLABS

In this section, the propagation of a plane wave through an infinite chiral nihility slab of thickness d is considered. The configuration for the chiral slab in a dielectric host medium is given in Fig. 7(a).

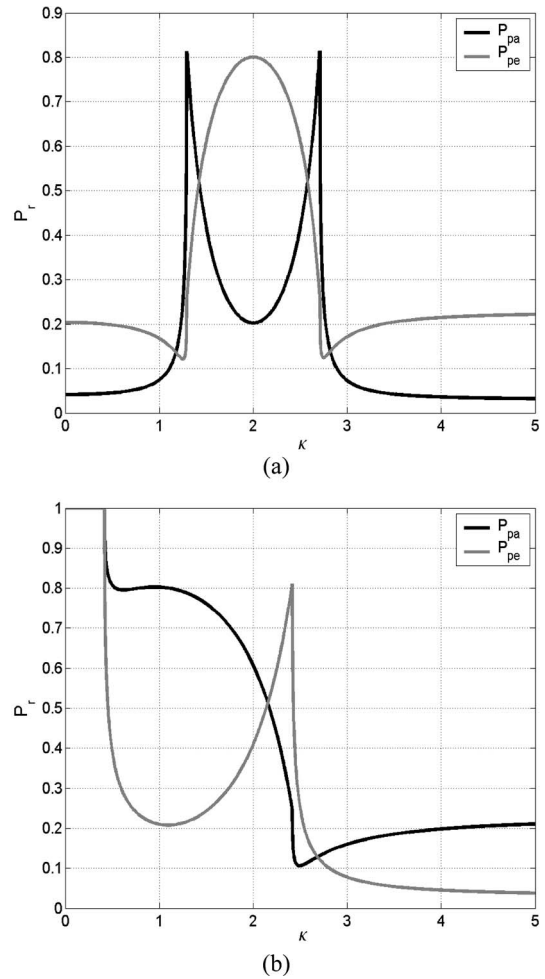


Fig. 5. Reflected power as a function of the chirality for an oblique incidence at an angle of $\theta_{inc} = 45^\circ$. (a) $\epsilon_1 = \mu_1 = 1$, $\epsilon = 4$, $\mu = 1$; (b) $\epsilon_1 = 4$, $\mu_1 = 1$, $\epsilon = \mu = 1$.

We assume that a plane wave propagating in a homogeneous isotropic dielectric medium is incident on the surface of a chiral slab defined by the constitutive relations of Eqs. (1) and (2). In our case, air is taken as the dielectric medium, and the two interfaces of the chiral slab are located at $z_n = 0$ and $z = d$. If we consider a frequency region where $\Re[\kappa] > \Re[\mu_r \epsilon_r]$, then one of the two waves is backward according to Eq. (5). Hence, for one of the two polarizations, the chiral medium will present a negative index of refraction, and in such a case subwavelength focusing will take place for waves of this polarization as shown in Fig. 7(b).

When $k_{inc} = k_r = k_t$, the angles of θ_1 and θ_2 (corresponding to the transmitted waves in the chiral slab) are given by

$$\theta_{1,2} = \sin^{-1} \left(\frac{k_{inc} \sin \theta_{inc}}{k_{1,2}} \right), \quad (11)$$

where $k_{inc} = k_0$, k_r , k_t denotes the incident, reflected, and transmitted wavenumbers, respectively. The boundary conditions of the tangential electric and magnetic fields are applied at the two interfaces situated at $z = 0$ and $z = d$, and a matrix form is then used to determine the reflected and transmitted fields in the presence of two inter-

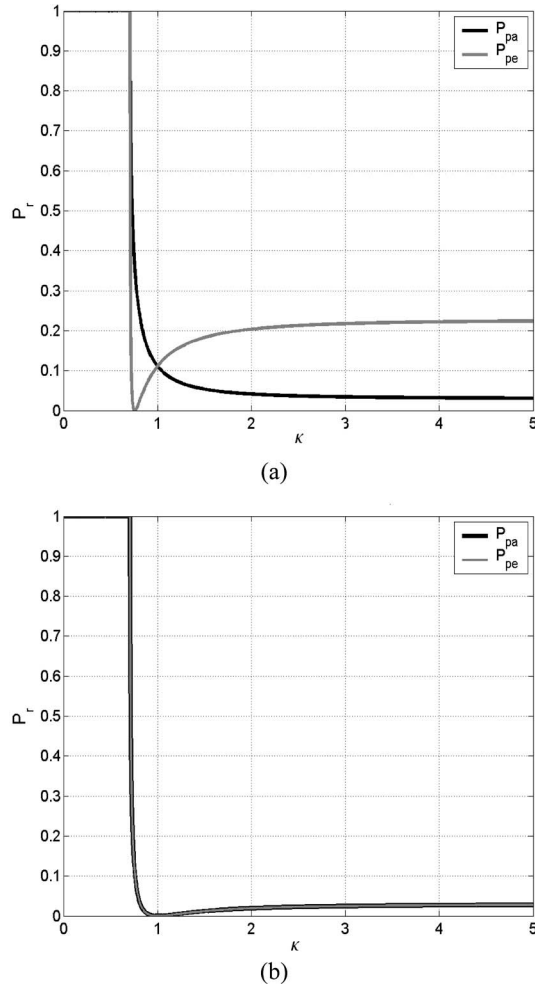


Fig. 6. Reflected power as a function of the chirality for an oblique incidence at an angle of $\theta_{inc}=45^\circ$ in different cases of chiral nihility. $\epsilon_1=\mu_1=1$. (a) $\mu_1=1 \times 10^{-5}$; (b) $\epsilon=\mu=1 \times 10^{-5}$.

faces of a chiral slab [24,25], based on the field decomposition [20] and the multiple scattering theories [26].

A. Modified Condition for Chiral Nihility

Now, we will revisit the chiral nihility. Let us now consider Born's relations [25,27] obtained from measurements:

$$\mathbf{D} = \frac{1}{1 - \epsilon_B \mu_B \gamma^2 k_0^2} (\epsilon_B \mathbf{E} + i \epsilon_B \mu_B \gamma k_0 \mathbf{H}), \quad (12)$$

$$\mathbf{B} = \frac{1}{1 - \epsilon_B \mu_B \gamma^2 k_0^2} (\mu_B \mathbf{H} - i \epsilon_B \mu_B \gamma k_0 \mathbf{E}), \quad (13)$$

where ϵ_B , μ_B , and γ denote the relative permittivity, relative permeability, and chirality, respectively, used by Born. One should note that the constitutive parameters used in Eqs. (1) and (2) can be expressed in terms of Born's parameters as follows:

$$\epsilon = \frac{\epsilon_B}{1 - \epsilon_B \mu_B \gamma^2 k_0^2}, \quad (14)$$

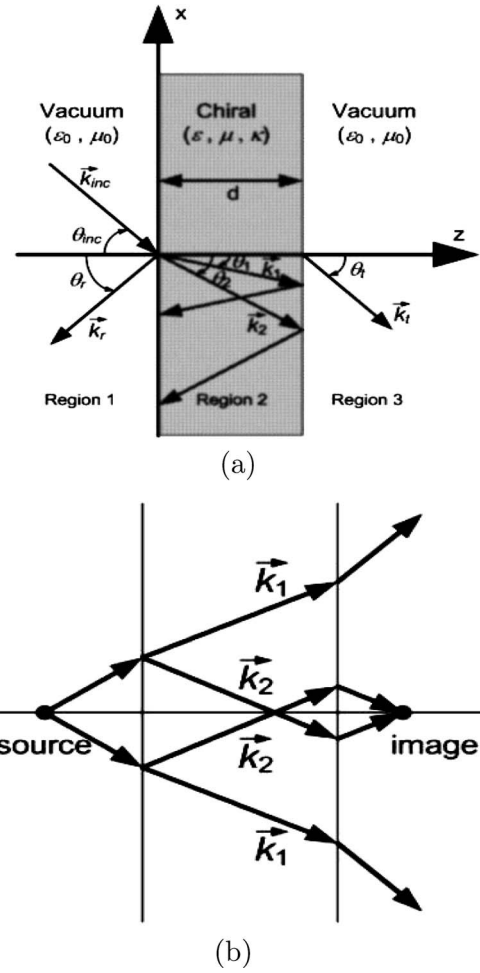


Fig. 7. (a) Chiral slab of thickness d placed in free space. The two interfaces with the chiral slab are situated at $z=0$ and $z=d$. Regions 1 and 3 are considered to be vacuum, and region 2 is the chiral medium. (b) Illustration of negative refraction and sub-wavelength focusing by a chiral slab ($k_1 > 0$ and $k_2 < 0$).

$$\mu = \frac{\mu_B}{1 - \epsilon_B \mu_B \gamma^2 k_0^2}, \quad (15)$$

$$\kappa = \frac{\epsilon_B \mu_B \gamma \omega}{(1 - \epsilon_B \mu_B \gamma^2 k_0^2)}. \quad (16)$$

In [19], the authors defined chiral nihility as medium parameters satisfying $\epsilon=0$, $\mu=0$, and $\kappa \neq 0$. When we apply these conditions to Born's parameters, however, we find that if $\epsilon=\mu=0$, then ϵ_B and μ_B must be both equal to zero, too. This restriction on ϵ_B and μ_B leads us to the fact that all the constitutive parameters are null regardless of the value of the Born chirality parameter γ . No propagation can be possible for such media, since Maxwell's equations become trivial, unless the γ in Eq. (16) approaches infinity. However, such a case lacks physical insight, since the corresponding chiral nihility requires $\epsilon_B=\mu_B=0$ and $\gamma \rightarrow \infty$.

Hence, in this paper we consider the chiral medium to have parameters $\epsilon_r=\mu_r=1 \times 10^{-5}$ (instead of zero) as an analogy to the modified condition of chiral nihility. Subsequently, it can be found that κ can take different values

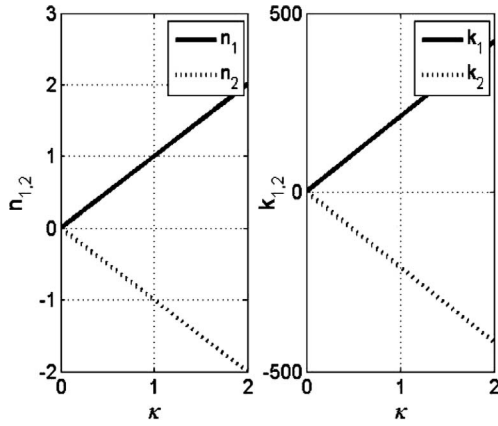


Fig. 8. Indices of refraction and wave vectors in the chiral nihility slab versus the chirality.

according to the values of γ . If the relation of $\epsilon_r = \mu_r = 1 \times 10^{-5}$ holds, ϵ_B and μ_B must also be equal to 1×10^{-5} . Concerning the chirality parameter, we have $\kappa \approx 2\pi\gamma$ at a frequency of 10 GHz. Since γ can take values only up to about unity [27], then an upper limit of 2π for κ is obtained here.

B. Numerical Results

First, we consider a chiral slab with both relative permittivity and relative permeability having values of 1×10^{-5}

(very close to 0) and the chirality parameter taking values between 0 and 2. We assume that the thickness of the slab along the z axis is $d=5$ mm ($0 < z < 5$ mm) and that a plane wave parallel to the plane of incidence [e.g., the yo z plane shown in Fig. 7(a)] coming from vacuum is incident on the chiral slab. The electric and magnetic field vectors are taken to be oriented along the x and y directions, respectively. The working frequency here is set to be 10 GHz. The magnitude of wave vector k and index of refraction n of each circularly polarized plane wave in a chiral nihility slab are plotted versus the chirality parameter in Fig. 8.

It is noted that when $\Re[\kappa] > \Re[\mu_r \epsilon_r]$, one of the two waves has a negative index of refraction, which corresponds to a backward wave in the chiral slab. For the whole set of values of κ , a matching of Z is achieved. But a matching of n with that of free space is achieved only for $\kappa=1$ in this particular case.

The transmitted power in vacuum on the right-hand side of a chiral nihility slab [region 3 of Fig. 7(a)] is plotted versus the angle of incidence θ_{inc} for different values of permittivity and permeability, and the results are shown in Fig. 9.

Two types of transmission are considered for the parallel incident plane wave, i.e., the nominal transmission, which is calculated from the ratio of the parallel transmitted E -field over the parallel incident E -field, and the cross

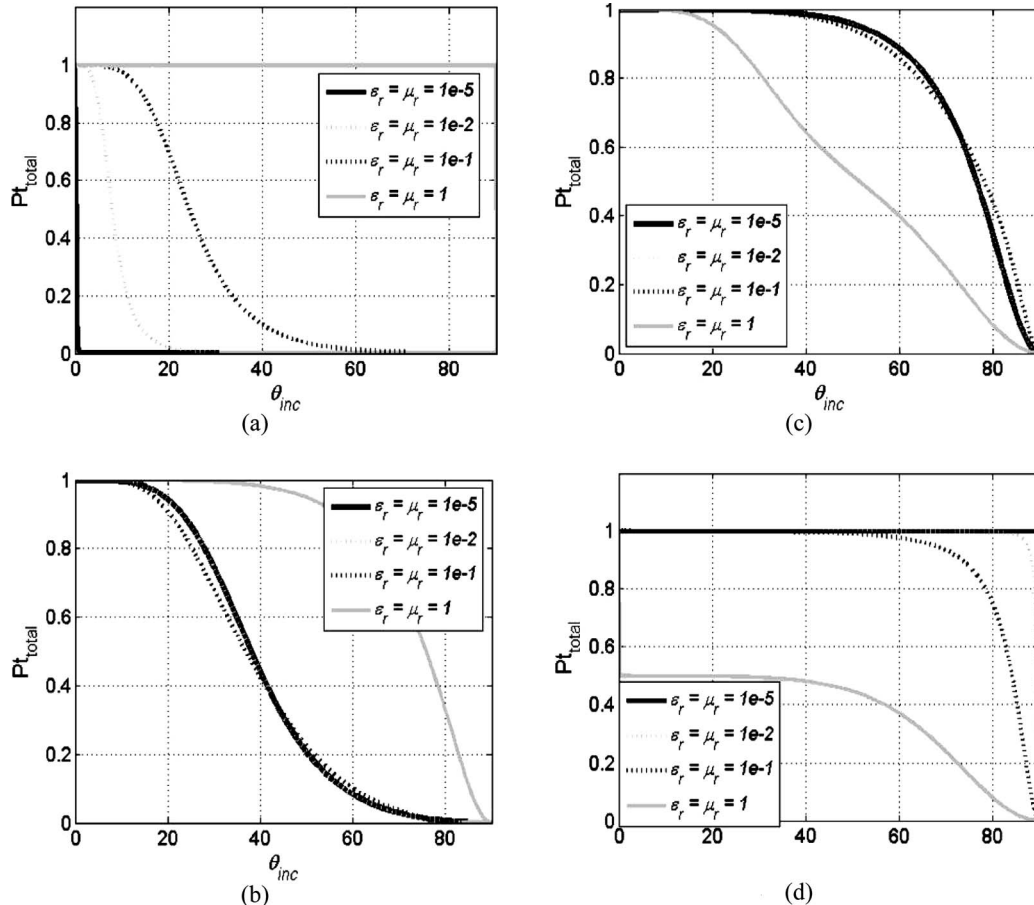


Fig. 9. Total transmitted power in vacuum on the right-hand side of the chiral nihility slab (region 3) for different values of ϵ_r and μ_r versus the angle of incidence θ_i . (a) $\kappa=0$, (b) $\kappa=0.25$, (c) $\kappa=0.8$, (d) $\kappa=1$.

transmission, which is calculated from the ratio of the perpendicular transmitted E -field over the parallel incident E -field.

It is noted from Fig. 9 that the total transmitted power depends strongly on the value of κ . For $\kappa=0$ (a normal dielectric medium), the transmitted power drops from 1 to 0 when the incident angle of the plane wave is slightly bigger than zero in the case where $\epsilon_r = \mu_r = 1 \times 10^{-5}$ [Fig. 9(a)]. For any oblique incidence, the power transmitted is null. When we simultaneously increase the values of ϵ_r and μ_r , a low-pass characteristic is observed; when $\epsilon_r = \mu_r = 1$ is reached, total transmission is obtained for the whole range of incidences varying from 0° to 90° , where a drop to zero is noted. If chirality is considered (e.g., $\kappa=0.25$), a low-pass characteristic is observed for each set of ϵ_r and μ_r values [Fig. 9(b)]. Increasing the values of ϵ_r and μ_r leads to a wider range of incident angles at which total transmission occurs. If we consider $\kappa=0.8$ [shown in Fig. 9(c)], we can still observe the low-pass characteristics, and the transmissions for $\epsilon_r = \mu_r = 1 \times 10^{-5}$ and $\epsilon_r = \mu_r = 1 \times 10^{-2}$ are the same. In the case of $\kappa=1$ and $\epsilon_r = \mu_r = 1 \times 10^{-5}$ [shown in Fig. 9(d)], the total transmitted power is unity at any angle of incidence between 0° and 90° , where it drops to zero. We should note that in this case one of the two eigenwaves in the chiral slab has a refractive index equal to -1 . For $\epsilon_r = \mu_r = 1 \times 10^{-2}$, the drop to zero transmission is smoother and occurs at a slightly lower incidence. A surprising phenomenon arises when $\epsilon_r = \mu_r = 1$ and $\kappa=1$. In fact, the total transmitted power drops drastically from 1 to 0.5 when the angle of incidence of the plane wave is zero. This is because only one eigenwave with $n=2$ propagates through the chiral medium. For an oblique incidence, from 0° to approximately 30° , only half of the total power is transmitted. At an angle of above 30° , there is a smooth drop till 90° , where the power transmitted is null. One possible and interesting application that needs to be mentioned in this particular case is a half-power divider for a selective range of incident angles.

Here, we consider the chiral nihility slab, and κ is assumed to be zero when $\epsilon_r = \mu_r = 1 \times 10^{-5}$ by considering $\gamma = 0$ in the Born formalism. To gain some insight into the behavior of the fields in different regions, the plots of the real and the imaginary parts of the E -field (E_x and E_z components) in these three regions are presented for the selected value parameters.

In Fig. 10, we show only the E_x component inside and outside the slab when a plane wave is normally incident (the E_z component is null at 0° incidence). Here, we notice that the imaginary and real parts of E_x are respectively null and unity inside the slab, and we also have conservation of energy inside the slab. We can observe that there exists no phase delay between the front face and the back face of the slab. This slab can then act as a phase compensator–conjugator. The slab is completely transparent to the electric field.

Assume now that the nihility slab has a chirality of 0.25. Then we still have the E_y component present, as shown in Fig. 11.

Note that here the two eigenwaves propagating inside the slab have an index of refraction equal to -0.25 and 0.25 . When $\kappa=0.25$, the real part of E_x decreases very slightly in the slab (region 2) with a normally incident

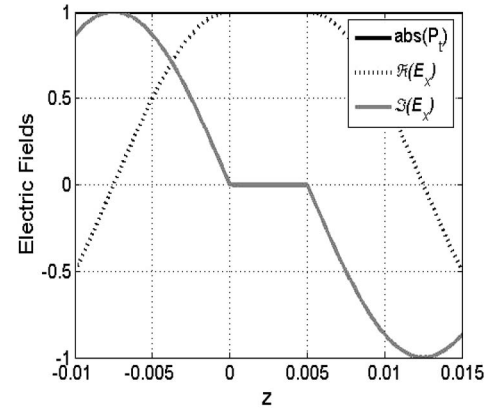
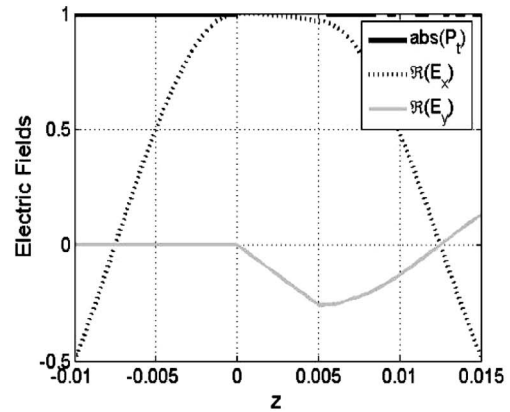
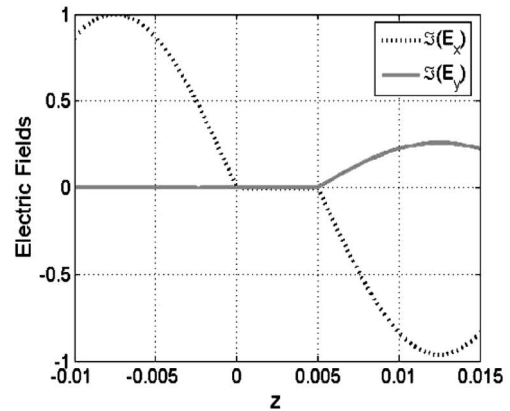


Fig. 10. Electric field and transmitted power as a function of the z coordinate when a normally incident wave illuminates a slab of medium with $\epsilon_r = \mu_r = 1 \times 10^{-5}$ and $\kappa=0$.

plane wave. The E_y component, which is null in region 1, increases linearly to 0.22 in the chiral slab. Concerning the imaginary parts presented in Fig. 11(b), we find that they are both equal to zero inside the slab and that there is no phase delay between the front and back faces of the slab. The cases studied in Figs. 10 and 11 are examples in which there is a matching of the wave impedance Z , since



(a)



(b)

Fig. 11. Electric field and transmitted power as a function of the z coordinate when a normally incident wave illuminates a slab of medium with $\epsilon_r = \mu_r = 1 \times 10^{-5}$ and $\kappa=0.25$. (a) Magnitude of real parts and transmitted power. (b) Magnitude of imaginary parts.

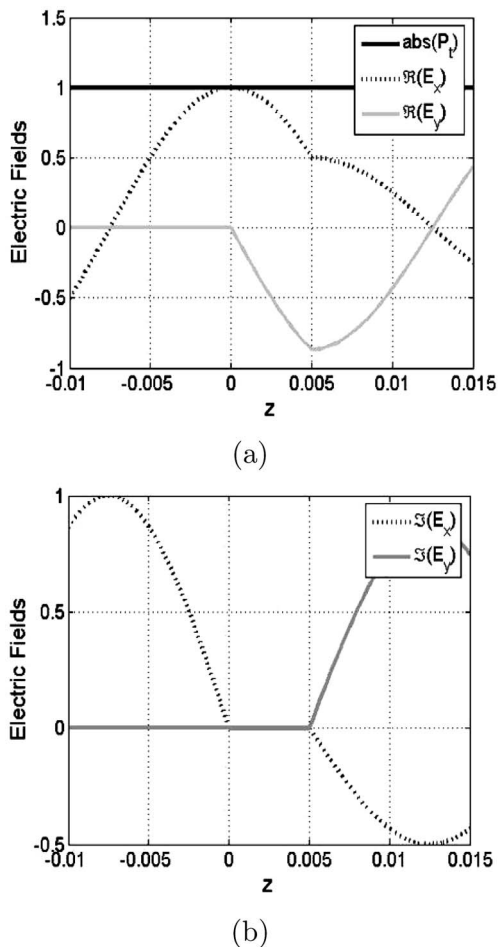


Fig. 12. Electric field as a function of the z coordinate when a normally incident wave illuminates a slab of medium with $\epsilon_r = \mu_r = 1 \times 10^{-5}$ and $\kappa = 1$. (a) Magnitude of real parts and transmitted power. (b) Magnitude of imaginary parts.

$\epsilon_r = \mu_r$, but not the refractive index n . In this section, a case of the matched refractive index is presented. Let us consider the case in which there is also a matched index of refraction by considering $\kappa = 1$. One of the two eigenwaves propagating in the slab will have $n = 1$, and the other will be a backward wave with $n = -1$. The electric field distribution of the normally incident plane wave is presented in Fig. 12.

Figure 12(a) shows that the real part of the E_y component takes quite high values in the slab because the cross transmission and the power transmitted in region 3 are equal to 1. Figure 12(b) shows that the imaginary part of E_y arises after the wave propagates through the slab, while it does not occur in regions 1 and 2. In this case, no phase delay can be observed.

4. CONCLUSION

In this paper, we have investigated a chiral nihility medium where both the permittivity and the permeability tend to zero. Some physical restrictions have been pointed out, and new conditions of chiral nihility have been proposed. The possibility of achieving a negative index of refraction and transparency in this medium has been verified numerically. Different components of the electric field

distribution in the chiral nihility slab placed in air have been presented. The dependence of chirality on the energy flow has been studied. It has been shown that the wave propagates in air without any phase delay, after passing through a chiral nihility slab. The slab physically behaves as a phase compensator or conjugator. A special case, where $\kappa = 1$, has been identified for a possible application of the slab as a half-power divider, where its peculiar properties of Brewster angles have been shown.

ACKNOWLEDGMENTS

The authors acknowledge the support of the SUMMA Foundation in the U.S. and the France–Singapore Merlion Project. The authors are grateful for support in part by a project from the U.S. Air Force Office of Scientific Research (FA4869-07-1-4024) and a research grant under the Academic Research Funds (ARC Tier-2) of the Ministry of Education, Singapore.

REFERENCES

1. V. G. Veselago, "The electrodynamics of substances with simultaneously negative values of ϵ and μ ," *Sov. Phys. Usp.* **10**, 509–514 (1968).
2. J. B. Pendry, A. J. Holden, W. J. Stewart, and I. Youngs, "Extremely low frequency plasmons in metallic meso structures," *Phys. Rev. Lett.* **76**, 4773–4776 (1996).
3. G. Fedorov, S. I. Maslovski, A. V. Dorofeenko, A. P. Vinogradov, I. A. Ryzhikov, and S. A. Tretyakov, "Subwavelength imaging: resolution enhancement using metal wire gratings," *Phys. Rev. B* **73**, 035409 (2006).
4. C. W. Qiu, H. Y. Yao, S. Zouhdi, L. W. Li, and M. S. Leong, "On the constitutive relations of G-chiral media and the possibility to realize negative-index media," *Microwave Opt. Technol. Lett.* **48**, 2534–2538 (2006).
5. H. Y. Yao, L. W. Li, C. W. Qiu, Q. Wu, and Z. N. Chen, "Properties of electromagnetic waves in a multilayered cylinder filled with double negative and positive materials," *Radio Sci.* **42**, 2006RS003509 (2006).
6. J. B. Pendry, "Negative refraction makes a perfect lens," *Phys. Rev. Lett.* **85**, 3966–3969 (2000).
7. J. B. Pendry, A. J. Holden, D. J. Robbins, and W. J. Stewart, "Magnetism from conductors and enhanced nonlinear phenomena," *IEEE Trans. Microwave Theory Tech.* **47**, 2075–2084 (1999).
8. R. A. Shelby, D. R. Smith, and S. Schultz, "Experimental verification of a negative index of refraction," *Science* **292**, 77–79 (2001).
9. N. Grigorenko, A. K. Geim, H. F. Gleeson, Y. Zhang, A. A. Firsov, I. Y. Khrushchev, and J. Petrovic, "Nanofabricated media with negative permeability at visible frequencies," *Nature* **438**, 335–338 (2005).
10. J. B. Pendry, "A chiral route to negative refraction," *Science* **306**, 1353–1355 (2004).
11. C. W. Qiu, H. Y. Yao, L. W. Li, S. Zouhdi, and T. S. Yeo, "Routes to left-handed materials by magnetoelectric couplings," *Phys. Rev. B* **75**, 245214 (2007).
12. X. Yang, T. X. Wu, and D. L. Jaggard, "Physical properties of wave scattering by a chiral grating," *J. Opt. Soc. Am. A* **21**, 2109–2116 (2004).
13. Q. Cheng and T. J. Cui, "Reflection and refraction properties of plane waves on the interface of uniaxially anisotropic chiral media," *J. Opt. Soc. Am. A* **23**, 3203–3207 (2006).
14. W. S. Weiglhofer and A. Lakhtakia, "Causality and natural optical activity (chirality)," *J. Opt. Soc. Am. A* **13**, 385–386 (1996).
15. S. Tretyakov, A. Sihvola, and L. Jylhä, "Backward-wave regime and negative refraction in chiral composites," *Photonics Nanostruct. Fundam. Appl.* **3**, 107–115 (2005).

16. F. A. Pinheiro and B. A. van Tiggelen, "Light transport in chiral and magnetochiral random media," *J. Opt. Soc. Am. A* **20**, 99–105 (2003).
17. M. P. Silverman and R. B. Sohn, "Effects of circular birefringence on light propagation and reflection," *Am. J. Phys.* **54**, 69–76 (1986).
18. S. Bassiri, C. H. Papas, and N. Engheta, "Electromagnetic wave propagation through a dielectric-chiral interface and through a chiral slab," *J. Opt. Soc. Am. A* **5**, 1450–1459 (1988).
19. S. Tretyakov, I. Nefedov, A. Sihvola, S. Maslovski, and C. Simovski, "Waves and energy in chiral nihility," *J. Electromagn. Waves Appl.* **17**, 695–706 (2003).
20. I. V. Lindell, A. H. Sihvola, S. A. Tretyakov, and A. J. Viitanen, *Electromagnetic Waves in Chiral and Bi-isotropic Media* (Artech House, 1994).
21. C. W. Qiu, L. W. Li, H. Y. Yao, and S. Zouhdi, "Properties of Faraday chiral media: green dyadics and negative refraction," *Phys. Rev. B* **74**, 115110 (2006).
22. C. W. Qiu, H. Y. Yao, L. W. Li, S. Zouhdi, and T. S. Yeo, "Backward waves in magnetoelectrically chiral media: propagation, impedance and negative refraction," *Phys. Rev. B* **75**, 155120 (2007).
23. M. P. Silverman, "Reflection and refraction at the surface of a chiral medium: comparison of gyrotropic constitutive relations invariant or noninvariant under a duality transformation," *J. Opt. Soc. Am. A* **3**, 830–837 (1986).
24. S. Zouhdi, "Étude des milieux chiraux aux fréquences micro-ondes. Calcul des paramètres constitutifs. Application aux motifs chiraux plans," Thèse de Doctorat (l'Université Pierre et Marie Curie, 1994).
25. A. Lakhtakia, *Beltrami Fields in Chiral Media*, Vol. 2 of World Scientific Series in Contemporary Chemical Physics (World Scientific, 1994).
26. J. A. Stratton, *Electromagnetic Theory* (McGraw-Hill, 1941).
27. M. Born, *Optik* (Springer-Verlag, 1930).